8th International Symposium on Magnetic Bearing
August 26-28, 2002, Mito, Japan

# EDDY CURRENT EFFECTS ON RADIAL ACTIVE MAGNETIC BEARINGS WITH SOLID ROTOR

**Yanhua Sun** **Lie Yu**
Theory of Lubrication and Bearing Institute
Xi'an Jiaotong Univ., Xi'an, Shaanxi, 710049 P.R. China
sunyanhua@tlbi.xjtu.edu.cn ,y ulie@xjtu.edu.cn

## ABSTRACT
This paper presents an analytical model to calculate eddy current losses, forces and stiffness of a radial magnetic bearing. A simplified bearing model is presented first. Then the analytical solutions of the magnetic field in the stator, air gap and rotor are obtained. Finally, the power loss could be achieved from the drag force acted on the rotor and the stiffness including eddy current effects from the radial force. It is found that the Reynolds number $R_m$ is a very important parameter to represent the rotation effects on the magnetic fields. The loss and the force could be transformed into nondimensional form with it. The results are verified with FEM analysis at last.

## INTRODUCTION
Eddy current is inevitable in the applications of active magnetic bearings (AMBs). The eddy current produced in the stator is induced by the varying control currents. But that produced in the rotor is caused both by the control currents and alternative changing of the static bias magnetic fields under the poles when rotating, and the later will be the main reason of the eddy current as the speed is high, especially when the heteropolar AMBs are used. Usually both the rotor and bearings are laminated to reduce the eddy current, but sometimes the solid rotor is still needed and the eddy current will be significant at high speed.

The first and most important effect of the eddy current is power loss. The eddy current loss in the rotating rotor will be dominant compared to the windage loss and hysteresis loss when the speed is high. Although it is always thought that magnetic bearing losses are lower than those of rolling element bearings and oil bearings, to predict it at the design stage is still important in the low loss high-speed applications such as energy storage system or spacecraft and satellite applications.

In the past decade, some studies on this subject have already been published in the open literature. Most of them aimed at either accurate measurement of the rotation losses or development of analytical or computational models for them. Kasarda etc. [1-3] had presented an analytical/empirical model that came from the power losses calculation of the transformer and electric machine. But it is difficult to calculate the effective frequencies and rotor volumes in this model accurately. Ahrens etc. [4] first introduced an analytical model based on magnetic field calculation to the eddy current loss in magnetic bearings with solid rotor. In this model, the magnetic field in the bearing was omitted and a steady magnetic flux distribution along the inner surface of the stator was assumed. But two dimensional (2D) FEM analysis [5-8] showed that the flux distribution under the poles changed by the eddy current as the speed is high. In fact, an analytical model including theef fect of eddy current on the main flux distribution under the poles could be achieved through magnetic field analysis if some simplifications on the bearings are performed.

In this paper, a simplified bearing model that derived from the model of Yoshimoto's FEM analysis [5,6] is presented first. Then the analytical solutions of the magnetic field in the stator, air gap and rotor are obtained similar to the approach in [4]. The power loss achieved from the drag force acted on the rotor and the stiffness including eddy current effects achieved from the radial force can be derived finally. At last, we have a FEM analysis to verify the analytical results achieved.

## MODEL SIMPLIFICATION
When a rotor rotates in a heteropolar radial magnetic bearing the direction of magnetic flux density in the air gap changes alternatively lookedfr om the rotor side.

Then the varying magnetic fields inside the rotor will induce eddy currents. Usually, the rotor is laminated to reduce the eddy currents, but it is difficult to develop an analytical model to get the actual three dimensional field distributions in the sheet in this case. Some kind of assumptions and simplifications should be done to get an approximate result [9,10]. The model in this paper is 2D, therefore it can only be used for solid rotor.

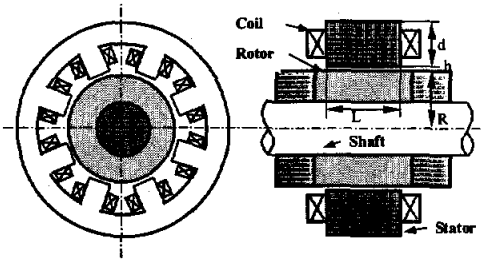


FIGURE 1: 8-pole radial magnetic bearing and rotor

The configuration of a solid rotor suspended by 8-pole magnetic bearing is shown in Figure 1. $R$ is the radius of the rotor, $h$ is the air gap, $d$ is the thickness of the back iron of the stator, and $L$ is the length of the bearing. All poles are assumed to be identical.

It is difficult, maybe impossible, to analytically solve Maxwell's equations in regions shown in Figure 1 because they are complicated too much. Therefore, the region of the stator must be simplified somewhat. In the analytical analysis of the magnetic fields of motors, it is always omitted the actual shape of the stator and use an equivalent surface current distribution as the boundary condition to represent the control currents. Yoshimoto also used this simplification in [5,6]. The stator was simplified to a ring and control currents in the coils were represented with an equivalent surface current distribution at the inner surface of the ring as shown in Figure 2 (a).

Since the magnetic field and the induced currents tend to concentrate at the surface of the rotor because of skin effect, the penetration depth of the magnetic field is far small than the radius of the rotor when the speed is high. Thus, the error of using Cartesian coordinates instead of cylindrical coordinates is small, and the rotor can then be approximated by a semi-infinite conducting plate as shown in Figure 2 (b).

In the following analysis, it is also assumed that the materials of the stator and rotor are linear and isotropy. Conductivity and permeability are assumed to be constant. Saturation and hysteresis effects are neglected.

The equivalent surface current distribution of an 8-pole heteropolar magnetic bearing is illustrated in Figure 3. The poles are arranged in NSNS configuration. $U_s = 2\pi(R+h)$ is the perimeter of the stator's inner surface. The surface current density can be approximated by a Fourier series:

$$J_0(x) = \sum_{n=1}^{\infty} (C_n e^{ik_n x} + \overline{C}_n e^{-ik_n x}) \qquad (1)$$

where $k_n = 2\pi n / U_s$

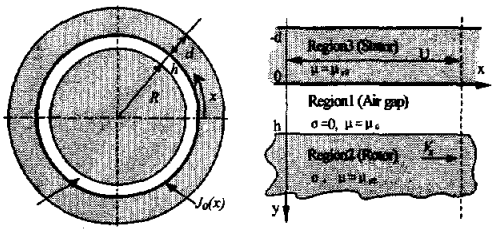


(a) (b)

(a) Regions for calculation
(b) Unrolled into Cartesian coordinates
FIGURE 2: Simplified model

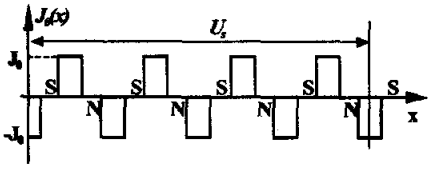


FIGURE 3: Equivalent surface current distribution

## MAGNETIC FIELDS

Maxwell's equation for the magnetic flux density inside the moving conducting material in steady state is:

$$\frac{1}{\mu\sigma}\nabla^2 B + \nabla \times (V \times B) = 0 \qquad (2)$$

where $V = \omega \cdot R$ is the speed of the rotor. The rotor is moving in $x$ direction, thus $V = V_x \vec{i}$. The flux density has only components in $x$ and $y$ direction, that is $B = B_x \vec{i} + B_y \vec{j}$, and the eddy currents are flowing in $z$ direction.

Since our analysis is linear, the field solution associated with each Fourier component of the current can be calculated separately and then summarized to get the whole solution. For simplicity, the following calculations in this section are only for one term $C_n e^{ik_n x}$, and all the subscript $n$ of the flux density $B$ are omitted. Using the similar method in [4], solutions of equation (2) in the region of air gap, rotor and stator can be derived.

In the air gap, $\sigma = 0$, $V_x = 0$, $q_n = k_n$, the solutions are:

$$B_{x1} = ie^{ik_n x}(a_1 e^{k_n y} - b_1 e^{-k_n y}) \qquad (3)$$

$$B_{y1} = e^{ik_n x}(a_1 e^{k_n y} + b_1 e^{-k_n y}) \qquad (4)$$

In the rotor, $q_n^2 = k_n^2 + ik_n \sigma_2 \mu_2 V_x$, the flux density are:

$$B_{x2} = b_2 \frac{q_n}{ik_n} e^{ik_n x} e^{-q_n y} \quad (5)$$

$$B_{y2} = b_2 e^{ik_n x} e^{-q_n y} \quad (6)$$

In the stator, $V_x = 0$, $q_n = k_n$,

$$B_{x3} = ie^{ik_n x}(a_3 e^{k_n y} - b_3 e^{-k_n y}) \quad (7)$$

$$B_{y3} = e^{ik_n x}(a_3 e^{k_n y} + b_3 e^{-k_n y}) \quad (8)$$

With the following boundary conditions at $y=0$ and $y=h$,

$$\frac{1}{\mu_1} B_{x1}\Big|_{y=0} - \frac{1}{\mu_3} B_{x3}\Big|_{y=0} = C_n e^{ik_n x}, B_{y3}\Big|_{y=-d} = 0$$

$$B_{y1}\Big|_{y=0} = B_{y3}\Big|_{y=0} \quad (9)$$

$$B_{y1}\Big|_{y=h} = B_{y2}\Big|_{y=h}, \frac{1}{\mu_1} B_{x1}\Big|_{y=h} = \frac{1}{\mu_2} B_{x2}\Big|_{y=h} \quad (10)$$

the five constants $a_1$, $b_1$, $b_2$, $a_3$ and $b_3$ which appear in equations can be obtained:

$$a_1 = C_n\left(1 - \frac{q_n}{\mu_{r2}k_n}\right)\frac{e^{-k_n h}}{2\gamma_{2,n}}, b_1 = C_n\left(1 + \frac{q_n}{\mu_{r2}k_n}\right)\frac{e^{k_n h}}{2\gamma_{2,n}}$$

$$b_2 = C_n \frac{e^{q_n h}}{\gamma_{2,n}}, a_3 = \frac{C_n}{1 - e^{-2k_n d}} \cdot \frac{\gamma_{1,n}}{\gamma_{2,n}}, b_3 = \frac{C_n}{1 - e^{2k_n d}} \cdot \frac{\gamma_{1,n}}{\gamma_{2,n}} \quad (11)$$

where

$$q_n^2 = k_n^2 + ik_n \sigma_2 \mu_2 V_x \quad (12)$$

$$\gamma_{1,n} = \cosh(k_n h) + \frac{q_n}{\mu_{r2} k_n} \sinh(k_n h) \quad (13)$$

$$\gamma_{2,n} = -\frac{i}{\mu_0}\left[\frac{\gamma_{1n}}{\mu_{r3}\tanh(k_n d)} + (\sinh(k_n h) + \frac{q_n}{\mu_{r2}k_n}\cosh(k_n h))\right] \quad (14)$$

## FORCES, LOSSE AND STIFFNESS

Using Maxwell's stress tensor, the magnetic forces acting on unit length of the rotor are:

$$F_x = -\frac{1}{\mu_0}\iint_s B_{x1} B_{y1} ds \quad (15)$$

$$F_y = -\frac{1}{2\mu_0}\iint_s (B_{y1}^2 - B_{x1}^2)\, ds \quad (16)$$

$s$ is any closed surface surrounding the conduct. For simplicity, the surface of the rotor is choused. Because of the orthogonality, each of the spatial harmonics integrates to zero when multiplied by each other, except where the two indices are the same. Hence, the forces from each harmonic can be considered separately and the results summed to get the total forces. The magnetic forces of a magnetic bearing with length $L$ are:

$$F_x = \frac{LU}{\mu_0 \mu_{r2}} \sum_{n=1}^{\infty} C_n \overline{C}_n \cdot \frac{i(q_n - \overline{q}_n)}{k_n} \cdot \frac{1}{\gamma_{2,n}\overline{\gamma}_{2,n}} \quad (17)$$

$$F_y = \frac{LU}{\mu_0 \mu_{r2}^2} \sum_{n=1}^{\infty} C_n \overline{C}_n \cdot \frac{q_n \overline{q}_n - \mu_{r2}^2 k_n^2}{k_n^2} \cdot \frac{1}{\gamma_{2,n}\overline{\gamma}_{2,n}} \quad (18)$$

Define the air gap ratio $\zeta$ and magnetic Reynolds number $R_m$ as follows:

$$\zeta = \frac{h}{R+h} \quad (19)$$

$$R_m = (R/\delta)^2 = R^2 \omega \mu_2 \sigma_2 / 2 \quad (20)$$

where $\delta = \sqrt{2/\omega\mu\sigma}$ is the skin depth. Then $q_n$ becomes

$$q_n = k_n \sqrt{1 + i2R_m / n} \quad (21)$$

Let

$$G_n = C_n \overline{C}_n / J_0^2 \quad (22)$$

$$H_n = \frac{\mu_{r2}^2 k_n^2 - q_n \overline{q}_n}{k_n^2} = \mu_{r2}^2 - \sqrt{1 + \frac{4R_m^2}{n^2}} \quad (23)$$

$$w_n(R_m) = -\frac{i(q_n - \overline{q}_n)}{k_n} = -i(\sqrt{1 + i2R_m/n} - \sqrt{1 - i2R_m/n}) \quad (24)$$

$$g_n(\zeta, R_m, \mu_{r2}) = \mu_0^2 \mu_{r2} \gamma_{2,n} \overline{\gamma}_{2,n} \quad (25)$$

Substituting (21) into (13) and (14) leads to

$$\gamma_{1,n} = \cosh(k_n h) + \frac{1}{\mu_{r2}} \sinh(k_n h) \sqrt{1 + i2R_m / n} \quad (26)$$

$$\gamma_{2,n} = -\frac{i}{\mu_0}[\sinh(k_n h) + \frac{\cosh(k_n h)}{\mu_{r3}\tanh(k_n d)} + \frac{1}{\mu_{r2}} \cdot (\cosh(k_n h) + \frac{\sinh(k_n h)}{\mu_{r3}\tanh(k_n d)})\sqrt{1 + i2R_m / n})] \quad (27)$$

$u_{r3}$ is very large, in the range of $10^3 \sim 10^5$, because the bearing is usually made of ferro materials, so $\sinh(k_n h) >> \cosh(k_n h)/(\mu_{r3}\tanh(k_n d))$ and $\cosh(k_n h) >> \sinh(k_n h)/(\mu_{r3}\tanh(k_n d))$. Therefore,

$$g_n(\zeta, R_m, \mu_{r2}) \approx \frac{\mu_{r2}}{2}[\cosh(2n\zeta) - 1] + \frac{1}{2}\sinh(2n\zeta) \cdot (\sqrt{1 + i2R_m/n} + \sqrt{1 - i2R_m/n}) + \frac{\cosh(2n\zeta) + 1}{2\mu_{r2}}\sqrt{1 + 4R_m^2/n^2} \quad (28)$$

Now the forces can be written as:

$$F_x = -J_0^2 LU \mu_0 \sum_{n=1}^{\infty} G_n \cdot \frac{w_n(R_m)}{g_n(\zeta, R_m, \mu_{r2})} \quad (29)$$

$$F_y = J_0^2 LU \frac{\mu_o}{\mu_{r2}} \sum_{n=1}^{\infty} \frac{G_n H_n}{g_n(\zeta, R_m, \mu_{r2})} \quad (30)$$

The minus in $F_x$ denote that it is a drag force and will prevent rotation of the rotor.

### Tangential force

Let

$$\psi(\zeta, R_m, \mu_{r2}) = \sum_{n=1}^{\infty} G_n \cdot \frac{w_n(R_m)}{g_n(\zeta, R_m, \mu_{r2})} \quad (31)$$

Then the tangential force $F_x$ becomes

$$F_x = -2\pi J_0^2 LR\mu_0 \psi(\zeta, R_m, \mu_{r2}) \quad (32)$$

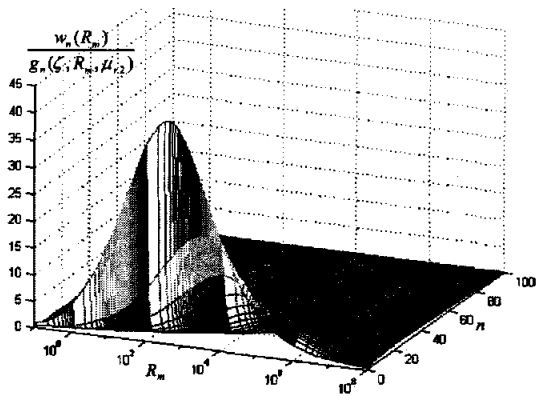


FIGURE 4: $w_n / g_n$

$\psi_i$ is the nondimensional drag force acting on unit area of the rotor by unit static surface current density. $G_n$ denotes the effect of different harmonic of the bias current, where $w_n / g_n$ represents effects of the speed, air gap ratio and material of the rotor.

The relation between $w_n / g_n$ and $n$ and $R_m$ is shown in Figure 4. For the nth harmonic, the tangential force rises sharply, peaks, and then decreases gradually. The drag force is the Lorentz force in fact. Its density is the vector $J \times B$. When $R_m$ is small the eddy current density is approximately proportional to $R_m$. So the tangential force increases rapidly. The skin effect becomes greater for large $R_m$. Though the eddy current density still increase, its distribution area minish rapidly. Therefore, the total force decreases when integrated in the area.

On the other hand, when $R_m$ is held constant, for small $R_m$, $w_n / g_n$ is decreasing rapidly as n increases, and peak will appear for large $R_m$. It means that effect of the low frequency components, especially the first two or three harmonics, is dominant when $R_m$ is small, and more and more harmonics will have effect as $R_m$ increases.

**Eddy current loss**

The power loss can be calculated with

$$P = F_x \cdot V_x \quad (33)$$

and written as

$$P = -L\frac{J_0^2}{\sigma_2} \cdot \Psi(\zeta, R_m, \mu_{r2}) \quad (34)$$

where $\Psi = 4\pi(R_m / \mu_{r2})\psi(\zeta, R_m, \mu_{r2})$ is the nondimensional loss of unit length and unit bias current density. When $R_m \to 0$, $g_n \approx \mu_{r2}(\cosh(2n\zeta) - 1)/2$ and $w_n \approx 2R_m / n$, therefore,

$$P = -4\pi J_0^2 LR^4 \omega^2 \mu_0^2 \sigma_2 \sum_{n=1}^{\infty} \frac{G_n}{n(\cosh(2n\zeta) - 1)} \propto \omega^2 \quad (35)$$

When $R_m$ is small $(1 \sim 10^3)$, $g_n \approx \mu_{r2}(\cosh(2n\zeta) - 1)/2$ and $w_n \approx 2\sqrt{R_m / n}$, then

$$P = -4\sqrt{2}\pi J_0^2 LR^3 \omega^{3/2} \mu_0^{3/2} \sqrt{\frac{\sigma_2}{\mu_{r2}}} \sum_{n=1}^{\infty} \frac{G_n}{\sqrt{n}(\cosh(2n\zeta) - 1)} \propto \omega^{3/2} \quad (36)$$

When $R_m \to \infty$, $g_n \approx (\cosh(2n\zeta) + 1)R_m / (n\mu_{r2})$ and $w_n \approx 2\sqrt{R_m / n}$, the loss will be

$$P = -4\sqrt{2}\pi J_0^2 LR\omega^{1/2} \sqrt{\frac{\mu_2}{\sigma_2}} \sum_{n=1}^{\infty} \frac{G_n \sqrt{n}}{(\cosh(2n\zeta) + 1)} \propto \omega^{1/2} \quad (37)$$

So the eddy current loss is proportional to the rotation speed squared ($\omega^2$) when $R_m$ approaches to zero, to $\omega^{3/2}$ when $R_m$ is small and to $\omega^{1/2}$ when $R_m$ approaches to infinity.

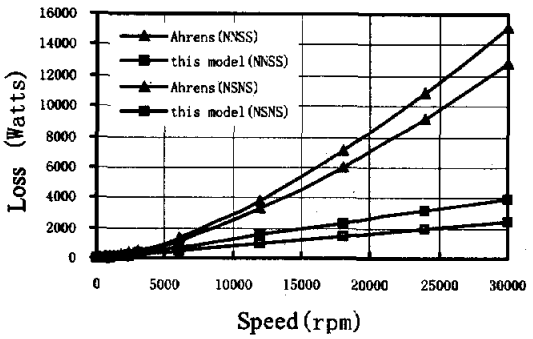


FIGURE 5: Loss compared with Ahrens' model

TABLE 1: Parameters of the rotor and bearing

| | |
|---|---|
| Outer radius of the stator | 98.1mm |
| Axial length | 43.6mm |
| Pole width | 21.1mm |
| Pole face area ratio | 58% |
| Ampere turns | 353A($B_0$=0.54T) |
| Radius of the rotor | 44.5mm |
| Air gap thickness | 0.762mm |
| Conductivity | $1.03\times10^7(\Omega m)^{-1}$ |
| Permeability | 2700 |

Ahrens [4] has assumed constant magnetic flux density at the boundary between the stator and the air gap and then got an analytical solution. But 2D FEM analysis [5-8] showed that the flux distribution under the poles changed by the eddy current as the speed is high. We have calculated the loss using Ahrens' model and ours with the parameters of the rotor and bearing in Table 1. The results are plotted in Figure 5. It can be

seen that Ahrens' model gives much higher eddy current loss than ours at high speed.

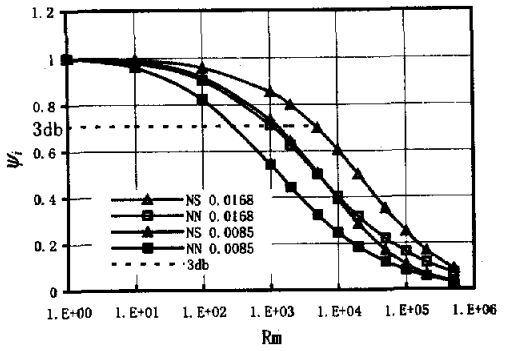


FIGURE 6: $\psi_i$ of an 8-pole bearing

TABLE 2: The parameters used to calculate $\psi_i$

| | | |
|---|---|---|
| $\zeta$ | Air gap ratio | 0.0168, 0.0085 |
| $\lambda$ | Pole face area ratio | 0.58 |
| $R$ | Radius of the rotor | 44.5mm |
| $u_{r2}$ | Relative permeability | 2700 |

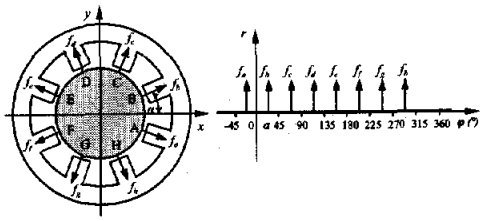

FIGURE 7: Radial force decomposition

**Radial force**

The radial force could be written as

$$F_r = F_y = F_{r0}\psi_i \tag{38}$$

$$\psi_i = \Psi_i / \Psi_{i0} \tag{39}$$

where $\Psi_i = \frac{1}{\mu_{r2}} \sum_{n=1}^{\infty} \frac{G_n H_n}{g_n(\zeta, R_m, \mu_{r2})}$ is a nondimentional quantity. $\Psi_{i0} = \Psi_i(R_m = 0)$ and $F_{r0} = J_0^2 LU\mu_0 \Psi_{i0}$ is the static radial force. $\psi_i$ is the normalized nondimensional radial force.

The force for an 8-pole bearing at different pole configurations (NNSS and NSNS) is plotted in Figure 6. The parameters used to calculate $\psi_i$ is in Table 2. Only the first 200 harmonics are used in calculation. It is indicated in figure that $R_m$ has little effect on $\psi_i$ when it is less than 100, but the radial force will decrease rapidly when $R_m$ is in the range of $10^2 \sim 2\times 10^5$. So the radial force will decrease dramatically at high speed.

**Stiffness**

The force derived in (38) is the total radial force of the bearing in Cartesian coordinate. Since all the poles are identical, the radial force of each pole is equal as shown in Figure 7. That is $f_a = f_b = \cdots = f_h = F_r/8$. Therefore, the force acting on the rotor in x direction will be:

$$f_x = f_a - f_e \quad \alpha \tag{40}$$

where $\alpha$ is half the angle between two poles.

If the bias current of each pole is $I_0$ and each coil has N turns, then the equivalent surface current density $J_0$ will be:

$$J_0 = NI_0 / l = KI_0 \tag{41}$$

where $l$ is half the length between two poles in circumference. If the poles are configured in differential manner, that is $I_a = I_b = I_0 + i$ and $I_e = I_f = I_0 - i$, then

$$f_x = I_0 i \cos\alpha K^2 LU\mu_0 \Psi_i \tag{42}$$

So the current stiffness is

$$k_i = \frac{\partial f_x}{\partial i}\Big|_{i=0} = I_0 \cos\alpha K^2 LU\mu_0 \Psi_i = k_{i0}\psi_i \tag{43}$$

where $k_{i0} = I_0 \cos\alpha K^2 LU\mu_0 \Psi_{i0}$ is the static stiffness and $\psi_i$ is the normalized nondimensional stiffness. Therefore, $\psi_i$ is both the normalized current stiffness and the normalized nondimensional radial force.

When the rotor moves from the center of the bearing, the air gap under each pole is unequal and not uniform anymore, then the radial force will change also. Assume that the displacement in $x$ direction is small and only the air gap under poles A, B, E and F changes, and the ununiform of the air gap can be neglected.

When the rotor has displacement $x$ in $x$ direction, the air gap under poles A and B will be $h$-$x$, and $h$+$x$ under poles E and F. Then the displacement stiffness will be

$$k_x = \frac{\partial f_x}{\partial x}\Big|_{x=0} = 2\left(\frac{\partial f_a}{\partial x} - \frac{\partial f_e}{\partial x}\right)\cos\alpha\Big|_{x=0} \tag{44}$$

where

$$\frac{\partial f_a}{\partial x} = -\frac{\partial f_e}{\partial x} = \frac{1}{8} J_0^2 LU\mu_0 \sum_{n=1}^{\infty} \frac{G_n H_n r_n(\zeta, R_m)}{g_n(\zeta, R_m)^2} \tag{45}$$

and

$$r_n(\zeta, R_m) = -\frac{k_n}{\mu_0^2}\left[\sinh(2n\zeta)\cdot\left(1 + \frac{1}{\mu_{r2}^2}\sqrt{1 + 4R_m^2/n^2}\right) + \frac{\cosh(2n\zeta)}{\mu_{r2}}\left(\sqrt{1 + i2R_m/n} + \sqrt{1 - i2R_m/n}\right)\right] \tag{46}$$

The displacement stiffness can be written as

$$k_x = k_{x0}\psi_x$$

$$\psi_x = \Psi_x \quad \Psi_x \tag{48}$$

where $\Psi_x = \frac{1}{2}\sum_{n=1}^{\infty} \frac{G_n H_n r_n(\zeta, R_m)}{g_n(\zeta, R_m)^2}$ is a nondimentional quantity, $\Psi_{x0} = \Psi_x(R_m = 0)$ and $k_{x0} = J_0^2 LU\mu_0 \Psi_{x0}\cos\alpha$ is the static displacement stiffness. $\psi_x$ is the normalized nondimensional displacement stiffness.

$\psi_x$ for an 8-pole bearing at different pole configurations is plotted in Figure 8. The parameters used to calculate $\psi_i$ is in Table 1 and only the first 200 harmonics are used in calculation. $\psi_x$ has the same property as $\psi_i$, but the range of $R_m$ in which $\psi_x$ decrease rapidly is $10^3 \sim 10^5$, smaller than that of $\psi_i$. The displacement stiffness will decrease at higher speed compared to $\psi_i$, but decrease more quickly.

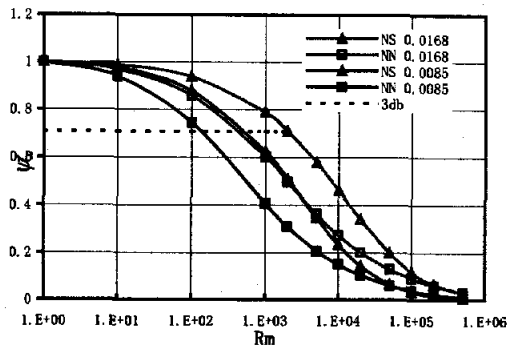


FIGURE 8: $\psi_x$ of an 8-pole bearing

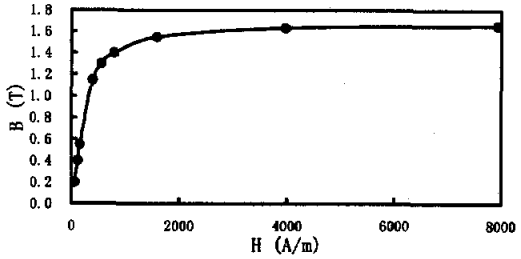


FIGURE 9: B-H curve

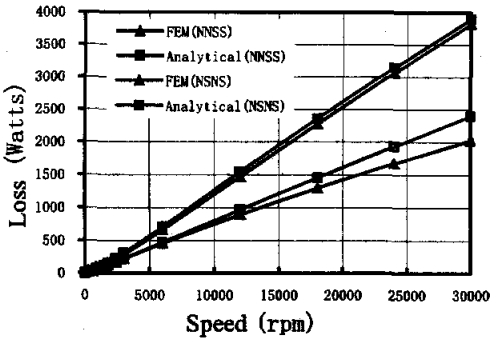


*FIGURE 10: Eddy current losses*

## FEM ANALYSIS

To verify the validity of those simplification and assumptions used in the analysis above, a numerical analysis is done on the actual bearing and rotor configuration pictured in Figure 1 using the FEM analysis software ANSYS5.6. The parameters of the rotor and bearing are in Table2. The B-H curve used in the nonlinear analysis is shown in Figure 9.

The losses derived from analytical model and the FEM analysis are plotted in Figure 10 and the radial forces in Figure 11. The stiffness is shown in Figure 12 and Figure 13. The analytical results agree well with the FEM results, so our model simplification and assumptions used in the analysis is reasonable. We also have a nonlinear FEM analysis considering the saturation of the magnetic field. The result shown that the saturation effect will make the radial force decrease at lower speed, hence enforces the eddy current effect.

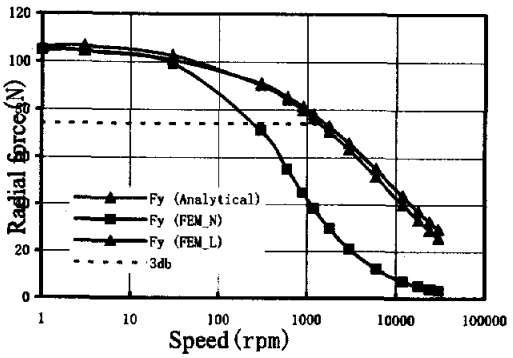


FIGURE 11: Radial forces

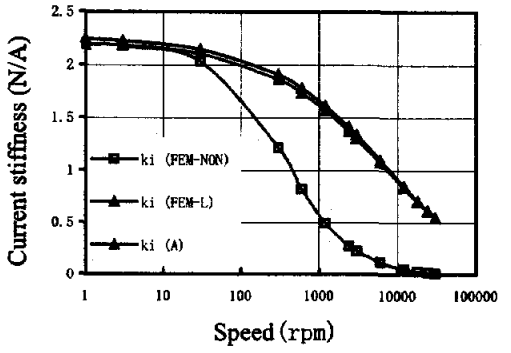


FIGURE 12: Current stiffness

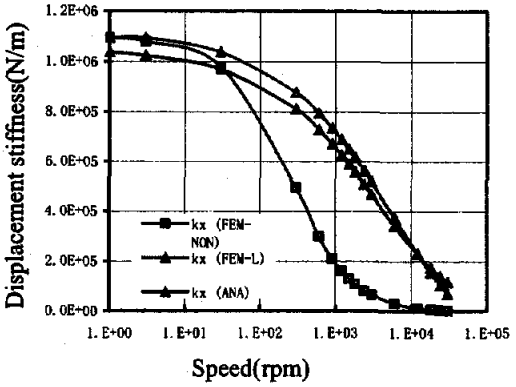


FIGURE 13: Displacement stiffness

## CONCLUSIONS

In this paper, the eddy current effects on rotor-active magnetic bearing system caused by rotation of the rotor are studied. A simplified bearing model and an equivalent current density distribution around the inner surface of the stator are presented first. Then the analytical solutions of the magnetic field in the stator, air gap and rotor are obtained. The magnetic forces acted on the rotor could be calculated Using Maxwell's stress tensor. Finally, the power loss achieved from the drag force acted on the rotor and the stiffness including eddy current effects achieved from the radial force can be derived.

It is found that the Reynolds number $R_m$, which denotes the effects of rotation speed, the conductance and permeability of the rotor, is a very important parameter to represent the effects of rotation on the magnetic fields. The loss and the force could then be transformed into nondimensional form with it.

The eddy current loss is proportional to the rotation speed squared ($\omega^2$) when $R_m$ approaches to zero, to $\omega^{3/2}$ when $R_m$ is small and to $\omega^{1/2}$ when $R_m$ approaches to infinity.

On the other hand, the eddy current will reduce forces acted on the rotor and cause the decrease of the stiffness of the bearing. An analytical model of the current/displacement stiffness of the bearing including eddy current effects is derived. It shows that the stiffness will decrease rapidly as $R_m$ increases.

The results achieved from the analytical model show good agreement with the FEM results based on the unsimplified bearing configuration.

**Acknowledgement**

This work was supported by the National Science Foundation of China under Grant 19990511 and National Project 863-2001AA411310.

**References**

1. M.E.F. Kasarda, P.E. Allaire, Comparison of Predicted and Measured Rotor Losses in Planar Radial Magnetic Bearings, Tribology Transactions, v 40, no2 1997, pp 219-226
2. M.E.F. Kasarda, P.E. Allaire, E.H. Maslen, G.R. Brown, G.T. Gillies, High Speed Rotor Losses in a Radial 8-pole Magnetic Bearing. Part 1: Experimental Measurement, Trans. of the ASME, Journal of Engineering for Gas Turbines and Power, v120, 1998, pp105-109
3. M.E.F. Kasarda, P.E. Allaire, P.M. Norris, etc., Experimentally Determined Rotor Power Losses in Homopolar and Heteropolar Magnetic Berings, Trans. of the ASME, Journal of Engineering for Gas Turbines and Power, v121, 1999, pp697-702
4. M. Ahrens, L. Kucera, Analytical Calculation of Fields, Forces and Losses of a Radial Magnetic Bearing with a Rotating Rotor Considering Eddy Currents. Proc. of the Fifth International Symposium on Magnetic Bearings, 1996, pp253-258
5. T. Yoshimoto, Eddy Current Effect in A Magnetic Bearing Model, IEEE Trans. on MAG, vol19,no.5, 1983, pp2097-2099
6. T. Yoshimoto, Effect of Nonlinear Permeability on Attractive Force and Counter Torque in a Magnetic Bearing Model, IEEE Trans. on MAG, vol20,No.5,1984, pp1959-1961
7. R.D. Rockwell, P. E. Allaire, J.C, Heinrich etc., Magnetic Field Finite Element Modeling of Magnetic Bearings Including Rotor Motion Effects and Eddy Currents, Proceedings of the 5th International Symposium on Magnetic Bearings. 1995, pp241-246
8. R.D. Rockwell, P. E. Allaire, M.E.F. Kasarda, Radial Plannar Magnetic Bearing Analysis with Finite Elements including Rotor Motion and Power Losses, Proceedings of the 1997 International Gas Turbine & Aeroengine Congress & Exposition, ASME, Jun 2-5 1997,
9. David C. Meeker, Eric H. Maslen, A Thin Plate Model for Predicting Rotating Losses in Magnetic Bearings, Proc. of Fifth Int'l. symp. on Magetic Bearings, 1996, pp247-252
10. Y. Sun, L. Yu, Analytical Method for Eddy Current Lloss in Lamminated Rotors with Magnetic Bearings, IEEE Tran. on Magnetics, Vol.38, No.2, 2002,pp1341-1347